Electronic Supplementary Material (ESI) for Dalton Transactions.
This journal is © The Royal Society of Chemistry 2022

Electronic Supplementary Information

Microporous chromium-organic framework fabricated via solvent-assisted metal metathesis for C_2H_2/CO_2 Separation

Ting-Ting Lu,[a] Ying-Yi Fan,[a] Xiao-Ning Wang*[a], Qiang Wang*[a], and Bao Li*[b]

[a] Hubei Key Laboratory of Biomass Fibers and Eco-dyeing & Finishing, School of Chemistry and Chemical Engineering, Wuhan Textile University, Wuhan, Hubei, 430200, P. R. China.

[b] Key Laboratory of Material Chemistry for Energy Conversion and Storage, School of Chemistry and Chemical Engineering, Hubei Key Laboratory of Bioinorganic Chemistry ＆Materia Medica, Huazhong University of Science and Technology, Wuhan, Hubei 430074, P. R. China.

* Corresponding Author

*E-mail: xnwang@wtu.edu.cn (X. N. Wang)

qiang_wang@wtu.edu.cn (Q. W.)

libao@hust.edu.cn (B. L.)

Synthesis of H_4L ligand

4,4’-diaminodiphenylsulfone (5g) had been added into 300 mL water containing potassium bromide (6 g) and potassium bromate (4.5 g). After stirring for 30 min, 8.5 mL concentrated HCl had been slowly added into the above mixture in two hours with strongly stirred at room temperature. The final mixture had been further stirred for two hours, and filtrated. The filter was washed with water for 5 times. After heated at 80 ℃ for one night, about 11g 3,3’,5,5’-Tetrabromo-4,4’-diaminodiphenylsulfone could be obtained.

To a solution of 3,3’,5,5’-Tetrabromo-4,4’-diaminodiphenylsulfone (4.3 g, 16.3 mmol), (4-(methoxycarbonyl)phenyl)boronic acid (7.0 g, 38.9 mmol) and K_3PO_4 (20.0 g, 94.2 mmol) in 1,4-dioxane (600 mL), $Pd(PPh_3)_4$ (1.4 g, 1.2 mmol) was added under nitrogen atmosphere. The resulting mixture was stirred at 100 °C for 48 h and then cooled to room temperature. After removing the organic solvent by rotary evaporation, dichloromethane (100 mL) and H_2O (50 mL) were added. The organic phase was separated and then the aqueous phase was extracted three times with dichloromethane (60 mL). The combined organic phases were washed with saturated brine, dried over anhydrous $MgSO_4$. After removing the organic solvent by rotary evaporation, the solid was dried at 80 °C in vacuum to give tetramethyl 5',5""-sulfonylbis(2'-amino-[1,1':3',1"-terphenyl]-4,4"-dicarboxylate) (4.1 g, 67.9%).

To a solution of tetramethyl 5',5""-sulfonylbis(2'-amino-[1,1':3',1"-terphenyl] -4,4"-dicarboxylate) (4.1 g, 11.0 mmol) in MeOH (100 mL) was added NaOH (1.5 g, 37.5 mmol). The resulting mixture was stirred at 80 °C overnight. After evaporation of MeOH, the aqueous residue was acidified with 2 M HCl to pH = 2~3. The resulting precipitate was filtered and washed with distilled water. The solid was dried at 80 °C in vacuum to give 5',5""-sulfonylbis(2'-amino-[1,1':3',1"-terphenyl]-4,4"-dicarboxylic acid) (3.4 g, 90.2%).^{1}H-NMR (400 MHz, DMSO-d_6): δ 7.96 (d, 4H, benzene-H), 7.45 (d, 4H, benzene-H), 7.48 (s, 2H, benzene-H).

Calculations of adsorption selectivity.

The pure-component isotherm data for CO_2, C_2H_2 and C_2H_4 were fitted with the

single-site Langmuir-Freundlich (LF) model:

$N = N_{max} \times (b \times p^{1/n} / (1 + b \times p^{1/n}))$

where p (unit: kPa) is the pressure of the bulk gas at equilibrium with the adsorbed phase, N (unit: mmol/g) is the adsorbed amount per mass of adsorbent, N_{max} (unit: mmol/g) is the saturation capacities, b (unit: 1/kPa) is the affinity coefficient and n represent the deviation from an ideal homogeneous surface.

Using the pure-component isotherm fits, the adsorption selectivity is defined by:

$$S_{ads} = \frac{q_1 / q_2}{p_1 / p_2}$$

Where q_i is the amount of i adsorbed and p_i is the partial pressure of i in the mixture.

Table S1. Crystal data of Fe-MOF

Fe-MOF	
Empirical formula	$C_{66}H_{40}Fe_3N_3O_{20}S_2$
CCDC number	2165343
Formula weight	1426.68
Crystal system	monoclinic
Space group	C2/*m*
a/Å	34.4082(10)
b/Å	26.2769(9)
c/Å	18.7449(6)
α/°	90
β/°	122.1830(10)
γ/°	90
Volume/Å^3	14344.0(8)
Z	4
ρ_{calc}g/cm^3	0.661
μ/mm^{-1}	0.460
F(000)	2908.0
Goodness-of-fit on F^2	1.193
Final R indexes [I>=2σ (I)]	R_1 = 0.0875, wR_2 = 0.2841
Final R indexes [all data]	R_1 = 0.1021, wR_2 = 0.2970
Largest diff. peak/hole / e Å^{-3}	0.79/-0.87

Table S2. ICP-MS results of sectional metal metathesis

	Fe-MOF	Cr-MOF
Cr (ug L^{-1})	0	278.1
Fe (ug L^{-1})	359.1	2.08
Cr/Fe ratio (%)	0	133.7

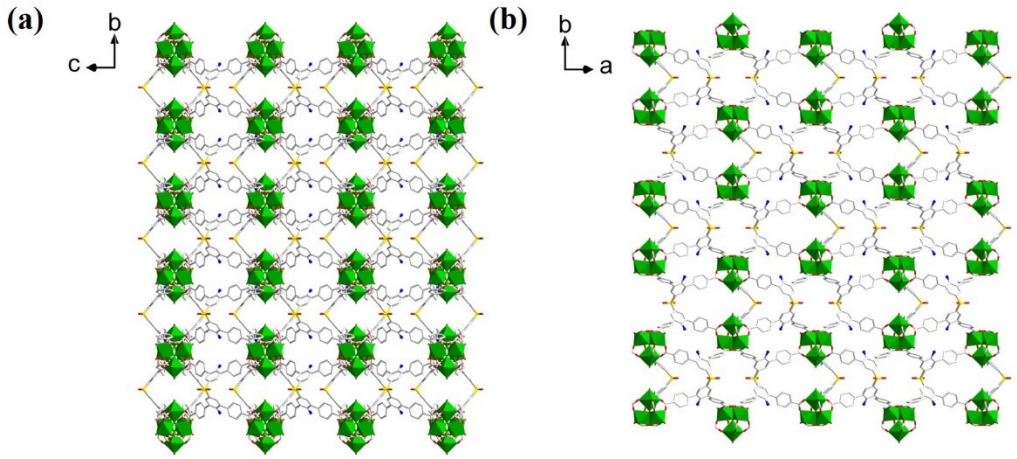

Figure S1. Partial view of 3D structure of Fe-MOF along a axis (a) and c axis (b).

Figure S2. Photo images of Fe-MOF and Cr-MOF.

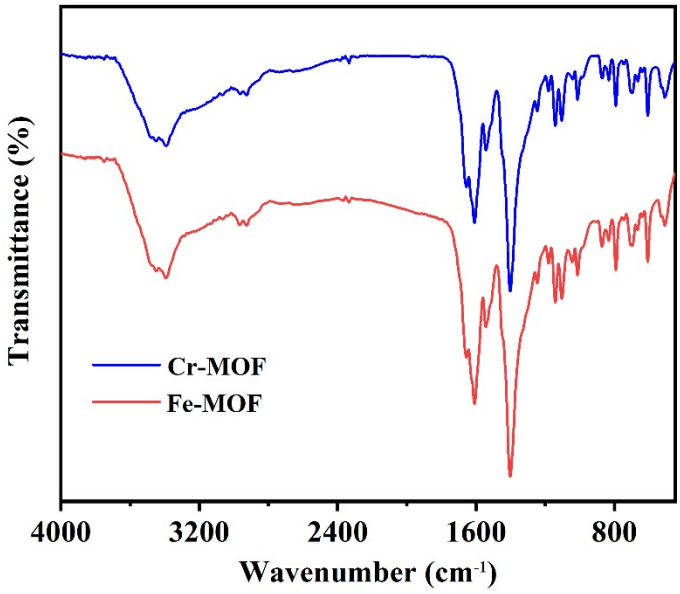

Figure S3. FTIR spectras of the as-prepared Fe-MOF and Cr-MOF.

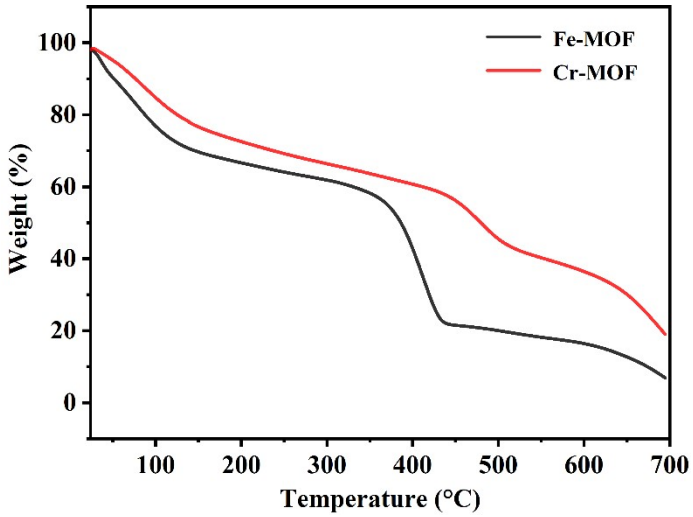

Figure S4. TGA curves of the as-prepared Fe-MOF and Cr-MOF.

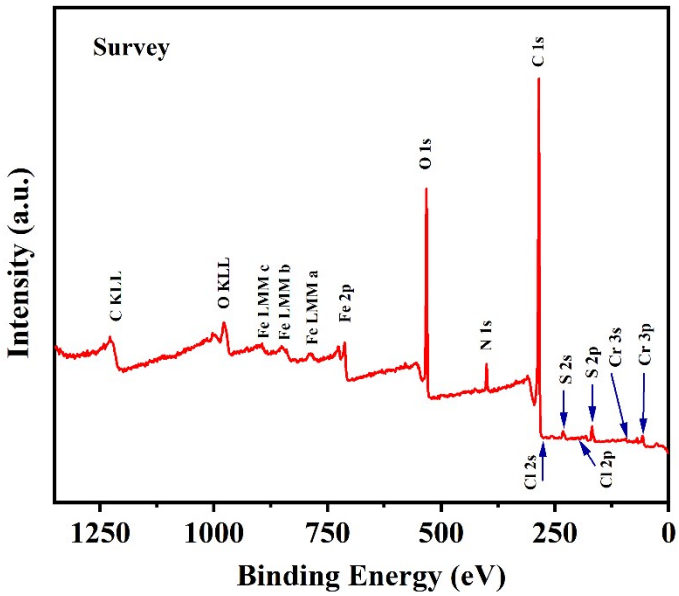

Figure S5. XPS survey spectra of Fe-MOF.

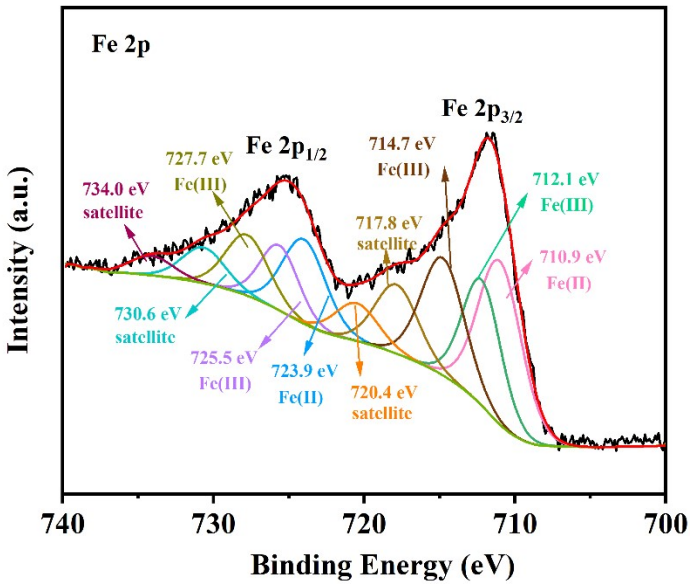

Figure S6. High-resolution XPS spectra of Fe 2p in Fe-MOF.

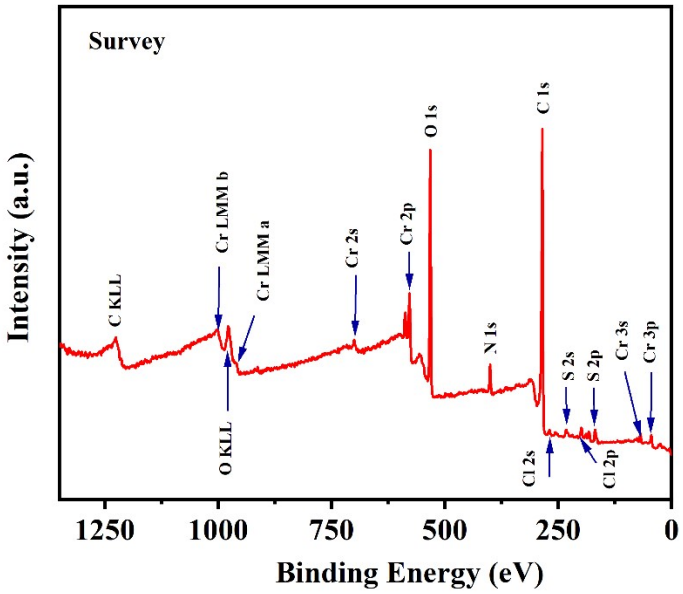

Figure S7. XPS survey spectra of Cr-MOF.

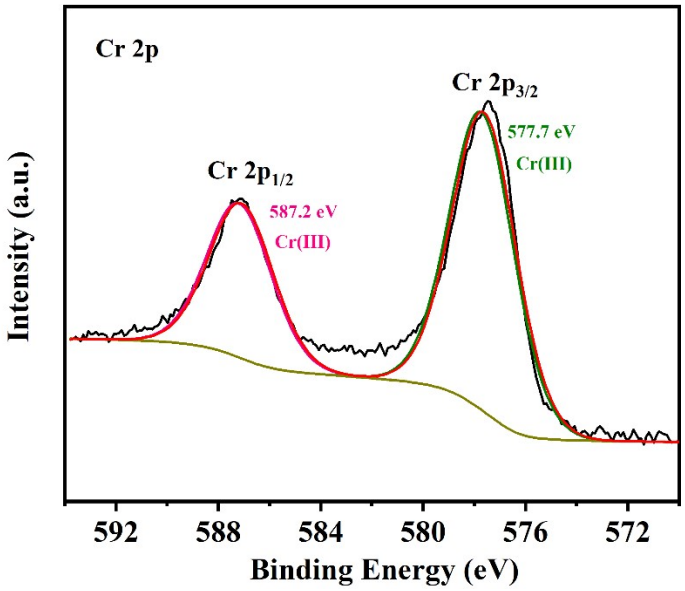

Figure S8. High-resolution XPS spectra of Cr 2p in Cr-MOF.

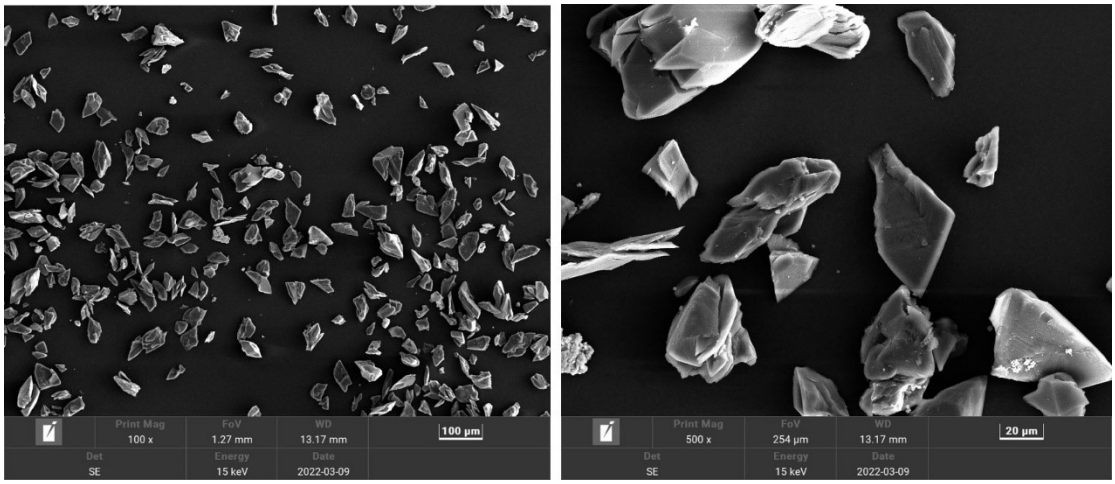

Figure S9. SEM images for Fe-MOF.

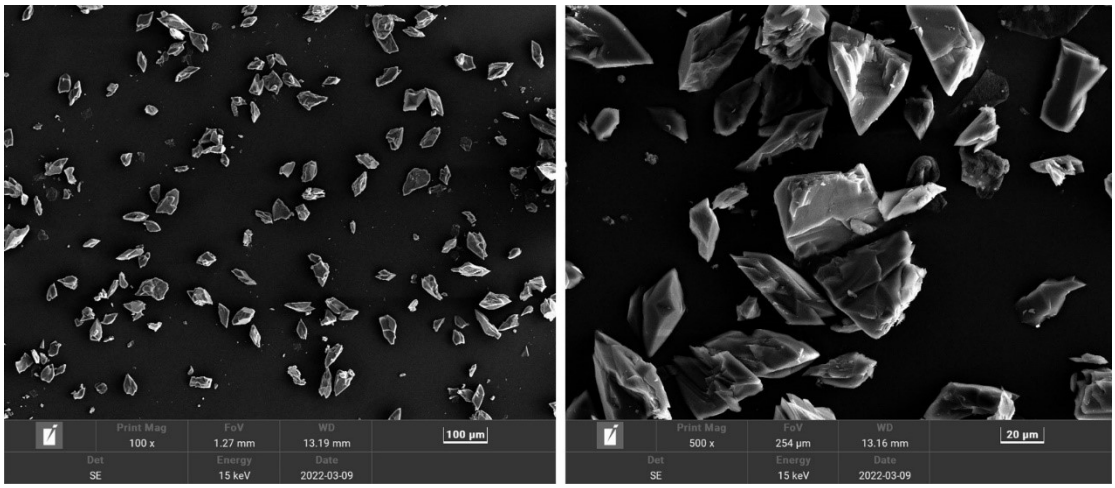

Figure S10. SEM images for Cr-MOF.

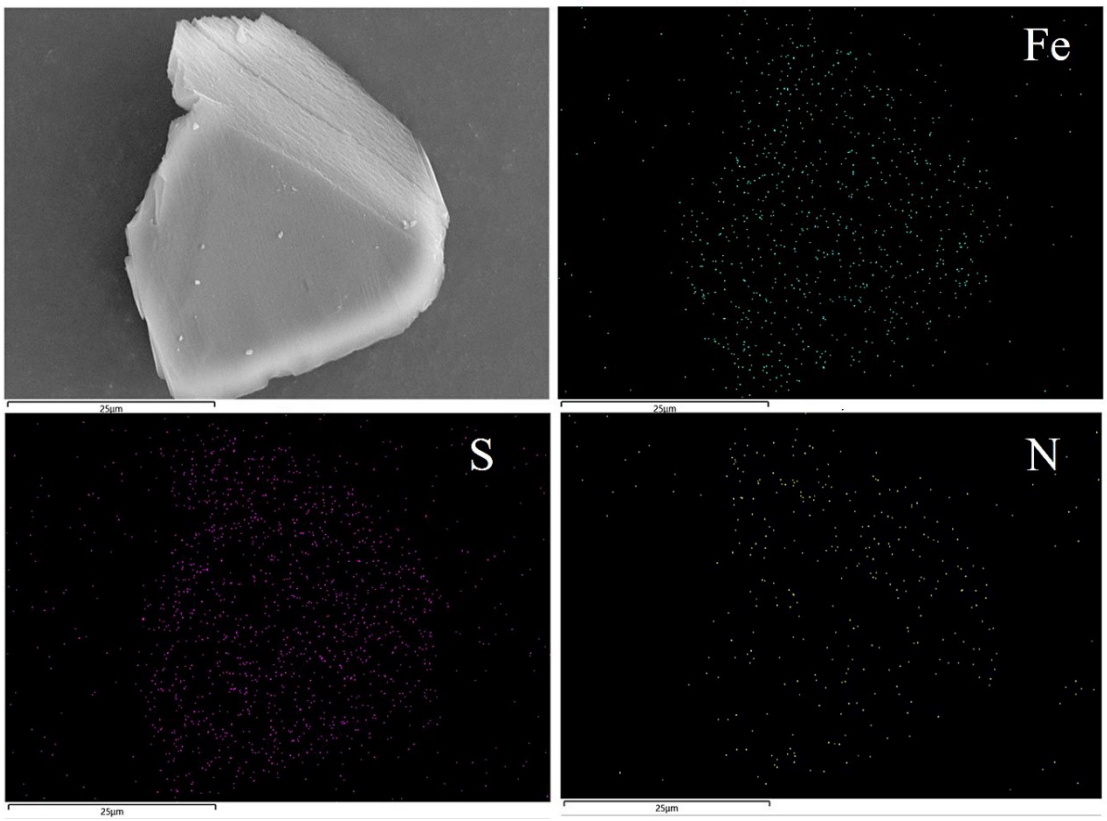

Figure S11. EDX images for Fe-MOF.

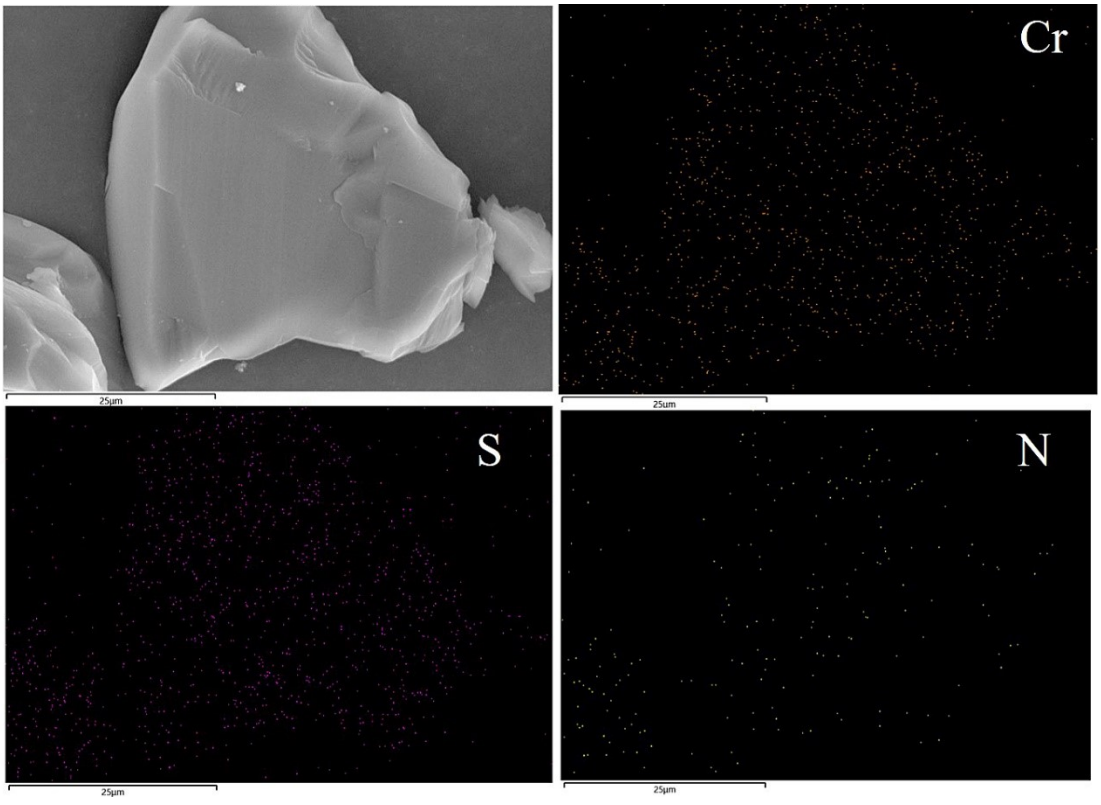

Figure S12. EDX images for Cr-MOF.

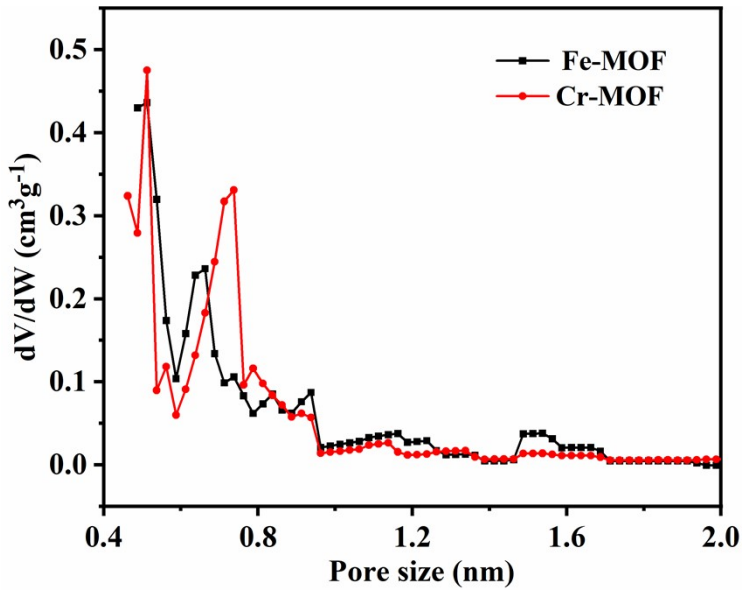

Figure S13. Pore size distributions of Fe-MOF and Cr-MOF.

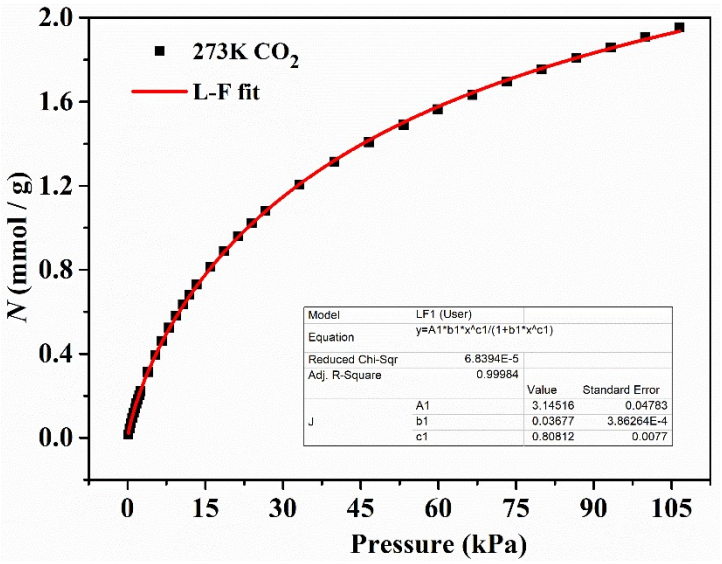

Figure S14. Langmuir-Freundlich fitting of the CO_2 sorption data at 273 K for Fe-MOF.

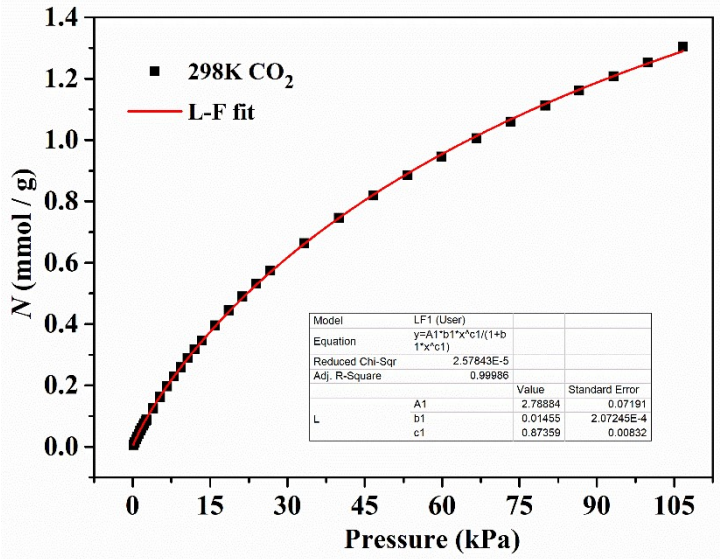

Figure S15. Langmuir-Freundlich fitting of the CO_2 sorption data at 298 K for Fe-MOF.

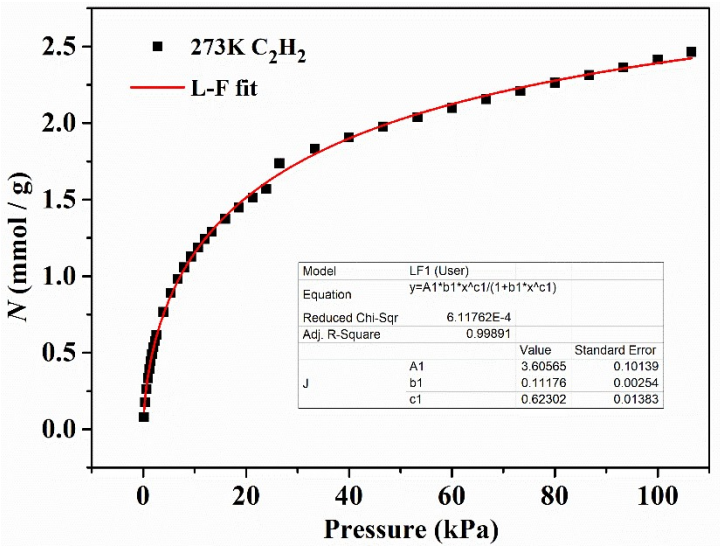

Figure S16. Langmuir-Freundlich fitting of the C_2H_2 sorption data at 273 K for Fe-MOF.

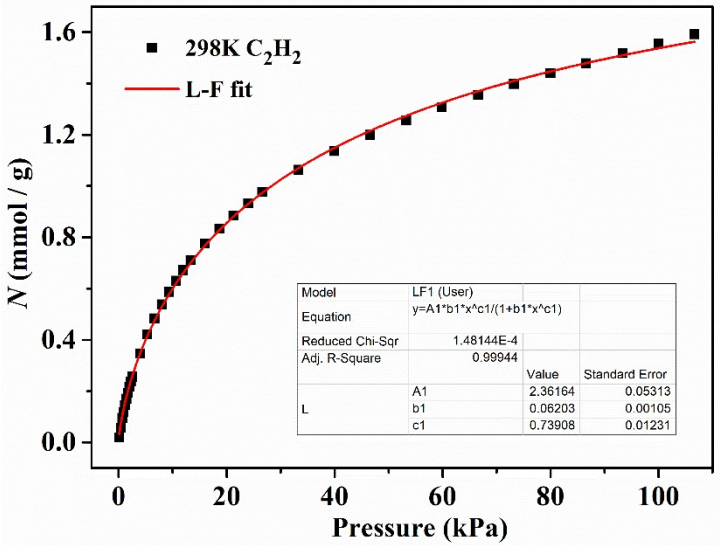

Figure S17. Langmuir-Freundlich fitting of the C_2H_2 sorption data at 298 K for Fe-MOF.

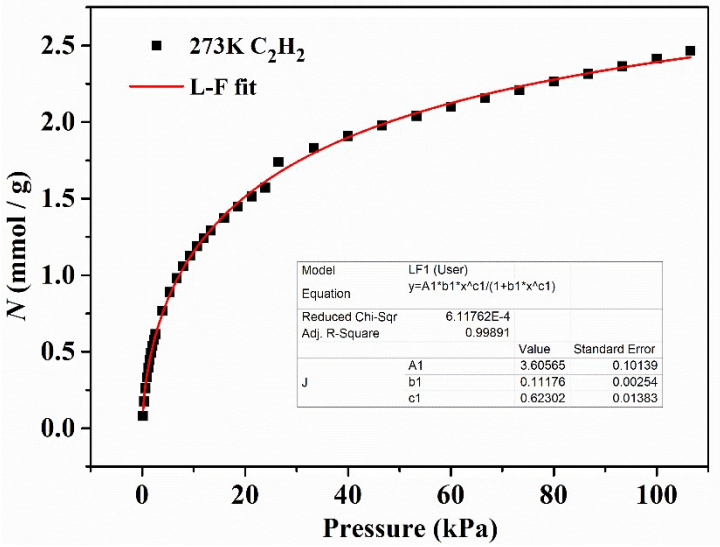

Figure S18. Langmuir-Freundlich fitting of the C_2H_2 sorption data at 273 K for Fe-MOF.

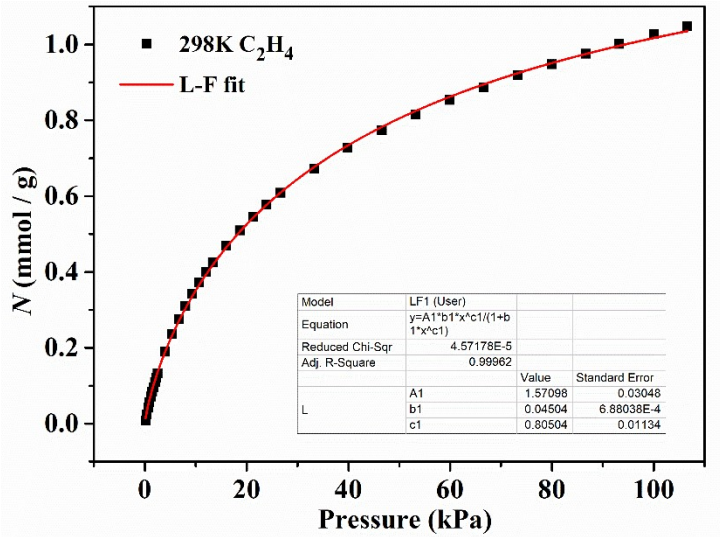

Figure S19. Langmuir-Freundlich fitting of the C_2H_4 sorption data at 298 K for Fe-MOF.

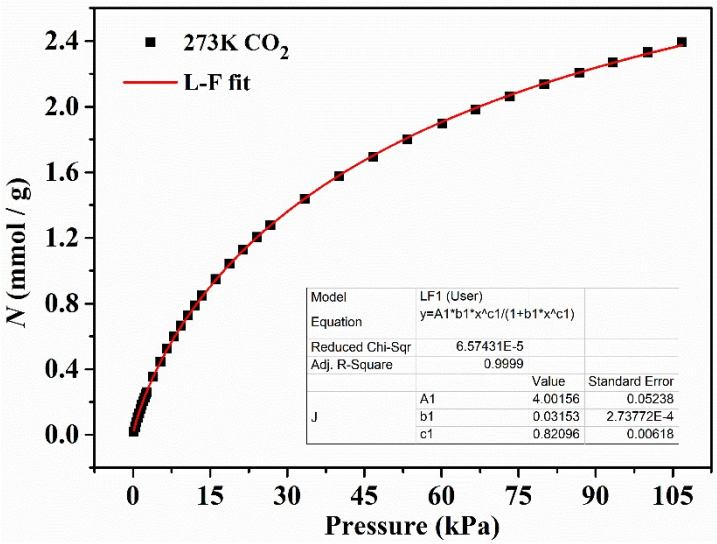

Figure S20. Langmuir-Freundlich fitting of the CO_2 sorption data at 273 K for Cr-MOF.

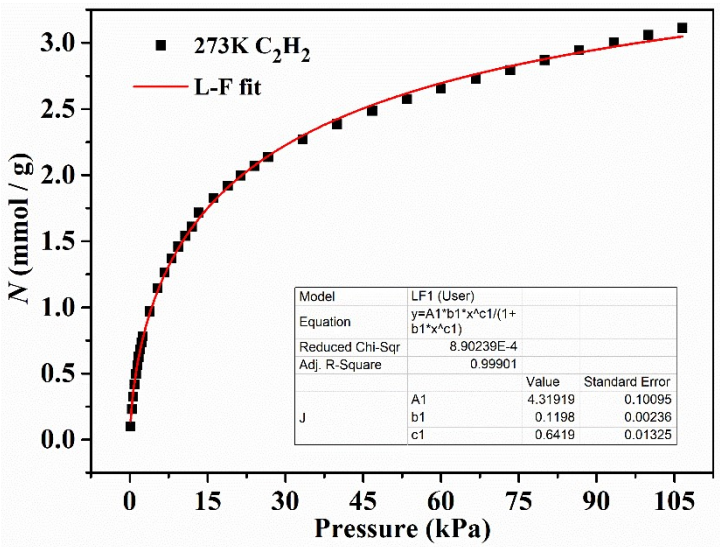

Figure S21. Langmuir-Freundlich fitting of the C_2H_2 sorption data at 273 K for Cr-MOF.

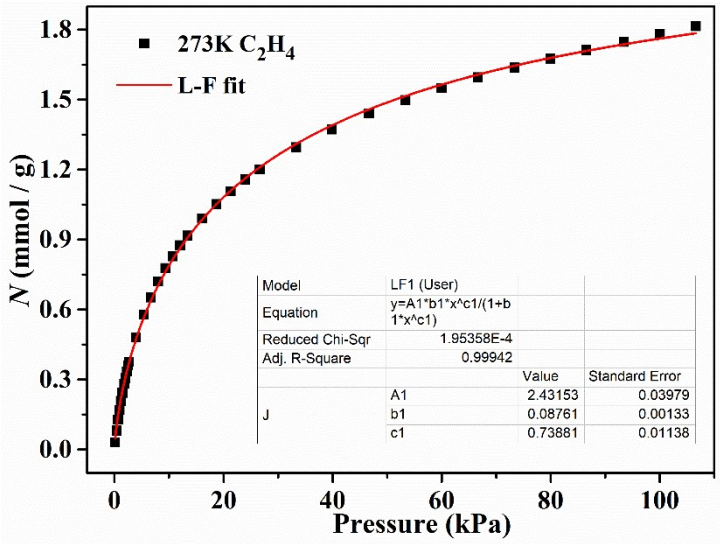

Figure S22. Langmuir-Freundlich fitting of the C_2H_4 sorption data at 273 K for Cr-MOF.

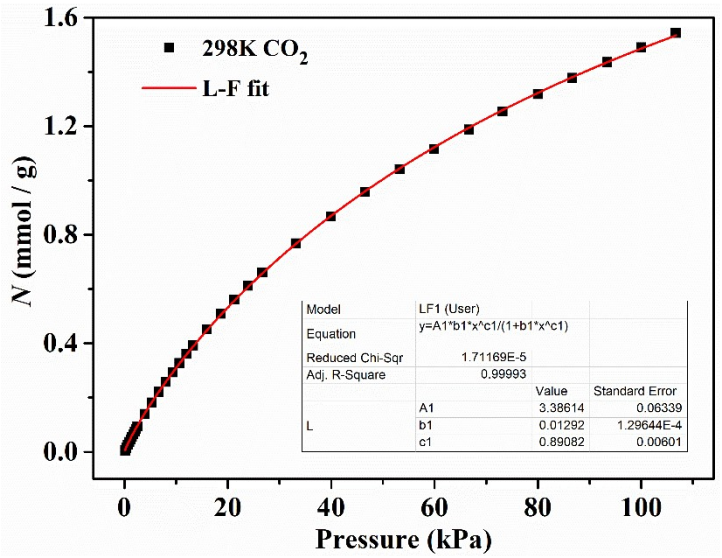

Figure S23. Langmuir-Freundlich fitting of the CO_2 sorption data at 298 K for Cr-MOF.

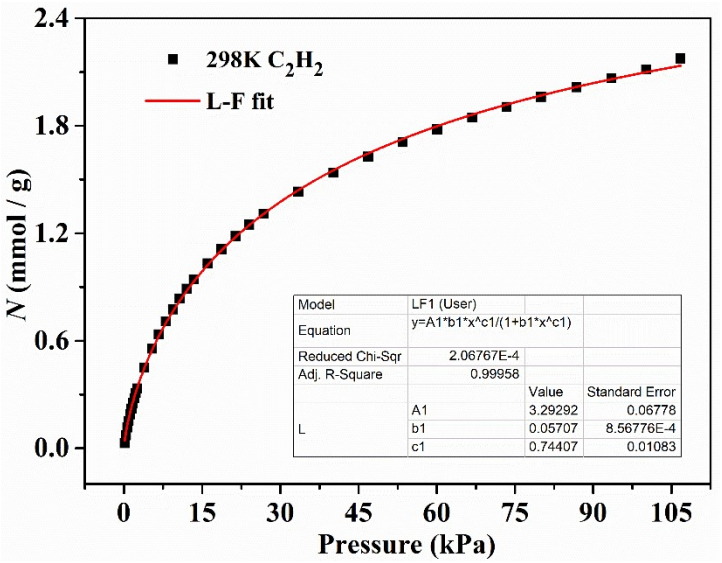

Figure S24. Langmuir-Freundlich fitting of the C_2H_2 sorption data at 298 K for Cr-MOF.

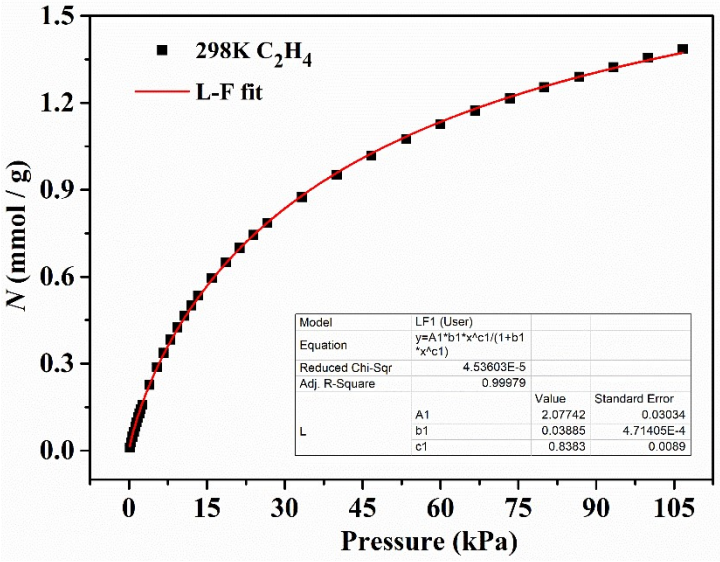

Figure S25. Langmuir-Freundlich fitting of the C_2H_4 sorption data at 298 K for Cr-MOF.

Table S3. A comparison of various MOFs materials used for selective adsorption for C_2H_2 over CO_2 and C_2H_4

MOFs materials	IAST calculated selectivity		Ref.
	C_2H_2/CO_2	C_2H_2/C_2H_4	
UPC-200(Al)-F-BIM	2.6		1
NOTT-300		2.3	2
MOF-74-Fe		1.87	3
UTSA-100a		10.72	4
FJU-36a	2.8		5
Cu-CPAH	3.6		6
SNNU-37(Fe)	9.9	2.4	7
SNNU-37(Sc)	2.7	1.7	7
FJU-90a	4.3		8
TIFSIX-2-Cu-i	6.5		9
UTSA-74a	9.0		10

SIFSIX-1-Cu		8.37	11
NbU-1		5.9	12
NbU-8		2.1	13
HUST-6		3.8	14
SNNU-45	4.5		15
UTSA-222	4.0		16
UTSA-30	3.4		17
UPC-112	2.8		18
ZJNU-100	3.8		19
Fe-MOF	2.7	2.9	This work
Cr-MOF	3.5	3.1	This work

References

(1) W. Fan, S. Yuan, W. Wang, L. Feng, X. Liu, X. Zhang, X. Wang, Z. Kang, F. Dai, D. Yuan, D. Sun and H. C. Zhou, *J. Am. Chem. Soc.*, 2020, **142**, 8728.

(2) S. Yang, A. J. Ramirez-Cuesta, R. Newby, V. Garcia-Sakai, P. Manuel, S. K. Callear, S. I. Campbell, C. C. Tang and M. Schröder, *Nat. Chem.*, 2014, **7**, 121.

(3) E. D. Bloch, W. L. Queen, R. Krishna, J. M. Zadrozny, C. M. Brown and J. R. Long, *Science*, 2012, **335**, 1606.

(4) T. L. Hu, H. Wang, B. Li, R. Krishna, H. Wu, W. Zhou, Y. Zhao, Y. Han, X. Wang, W. Zhu, Z. Yao, S. Xiang and B. Chen, *Nat. Commun.*, 2015, **6**, 7328.

(5) L. Liu, Z. Yao, Y. Ye, L. Chen, Q. Lin, Y. Yang, Z. Zhang and S. Xiang, *Inorg. Chem.*, 2018, **57**, 12961.

(6) L. Meng, L. Yang, C. Chen, X. Dong, S. Ren, G. Li, Y. Li, Y. Han, Z. Shi and S. Feng, *ACS Appl. Mater. Interfaces*, 2020, **12**, 5999.

(7) S. C. Fan, Y. T. Li, Y. Wang, J. W. Wang, Y. Y. Xue, H. P. Li, S. N. Li and Q. G. Zhai, *Inorg. Chem.*, 2021, **60**, 18473.

(8) Y. Ye, Z. Ma, R. B. Lin, R. Krishna, W. Zhou, Q. Lin, Z. Zhang, S. Xiang and B. Chen, *J. Am. Chem. Soc.*, 2019, **141**, 4130.

(9) K. J. Chen, H. S. Scott, D. G. Madden, T. Pham, A. Kumar, A. Bajpai, M. Lusi, K.

A. Forrest, B. Space, J. J. Perry and M. J. Zaworotko, *Chem.* 2016, **1**, 753.

(10) F. Luo, C. Yan, L. Dang, R. Krishna, W. Zhou, H. Wu, X. Dong, Y. Han, T. L. Hu, M. O'Keeffe, L. Wang, M. Luo, R. B. Lin and B. Chen, *J. Am. Chem. Soc.*, 2016, **138**, 5678.

(11) X. Cui, K. Chen, H. Xing, M. J. Zaworotko and B. Chen, *Science*, 2016, **353**, 141.

(12) J. Li, L. Jiang, S. Chen, A. Kirchon, B. Li, Y. Li and H. C. Zhou. *J. Am. Chem. Soc.*, 2019, **141**, 3807.

(13) Q. Li, N. Wu, J. Li and D. Wu, *Inorg. Chem.*, 2020, **59**, 13005.

(14) F. Yu, B. Q. Hu, X. N. Wang, Y. M. Zhao, J. L. Li, B. Li and H. C. Zhou, *J. Mater. Chem. A*, 2020, **8**, 2083.

(15) Y. P. Li, Y. Wang, Y. Y. Xue, H. P. Li, Q. G. Zhai, S. N. Li, Y. C. Jiang, M. C. Hu and X. Bu, *Angew. Chem. Int. Ed.*, 2019, **58**, 13590.

(16) J. Ma, J. Guo, H. Wang, B. Li, T. Yang and B. Chen, *Inorg. Chem.*, 2017, **56**, 7145.

(17) Y. He, S. Xiang, Z. Zhang, S. Xiong, F. R. Fronczek, R. Krishna, M. OQKeeffe and B. Chen, *Chem. Commun.*, 2012, **48**, 10856.

(18) W. Fan, X. Wang, X. Liu, B. Xu, X. Zhang, W. Wang, X. Wang, Y. Wang, F. Dai, D. Yuan and D. Sun, *ACS Sustainable Chem. Eng.*, 2019, **7**, 2134.

(19) Y. Wang, M. He, X. Gao, X. Wang, G. Xu, Z. Zhang and Y. He, *Inorg. Chem. Front.*, 2019, **6**, 263.